

Role of ambient pressure on bouncing and coalescence of colliding jets

Minglei Li,^{1,2} Abhishek Saha,^{3,2,*} Chao Sun,¹ and Chung K. Law^{2,1}

¹*Center for Combustion Energy, Tsinghua University, Beijing 100084, China*

²*Department of Mechanical and Aerospace Engineering,
Princeton University, Princeton, NJ 08544, USA*

³*Department of Mechanical and Aerospace Engineering,
University of California San Diego, La Jolla, CA 92093, USA*

(Dated: June 21, 2023)

In this letter, the merging-vs-bouncing response of obliquely-oriented colliding jets under elevated and reduced gaseous environment pressures was experimentally examined. Experiments with water and n-tetradecane confirmed that the collision outcome transitions from merging to bouncing, and then to merging again, when the impact velocity was increased. This behavior which was previously reported for atmospheric pressure, has now also been observed at elevated and reduced pressures. New results also show that there exists a critical pressure (0.9 bar for tetradecane and 5 bar for water) below which increasing pressure promotes bouncing (expands the bouncing regime), while beyond this, merging is promoted (reduces the bouncing regime) instead. This leads to a non-monotonic influence of pressure on the non-coalescence outcomes of collisional jets, which was not previously reported. The study provides evidence of new behaviors in colliding jets at reduced and elevated pressures, which differs from well-studied droplet-droplet collisions.

Collision of two liquid masses in gaseous environments is a frequently occurring event in many natural and industrial processes, for example in cloud and raindrop formation as well as spray and mixing processes within liquid-fueled combustors such as diesel and rocket engines [1–7]. It has been found that the colliding masses, such as droplet-droplet [8–11], droplet-film [12–15] and jet-jet [16, 17], could result in non-coalescence and hence bouncing outcomes instead of merging as nominally expected. The cause for the non-coalescence response is the presence of the intervening gas layer between the impacting liquid masses, which can be as thin as tens to hundreds of nanometers [18–21] and needs to be “squeezed” out by the impacting liquid surfaces before the impact momentum is dissipated. In particular, it has been conclusively demonstrated, for both the droplet and jet systems, that with increasing impact inertia, the collision response can evolve from merging to bouncing to merging again and finally to merging, followed by disintegration of the merged mass. For conceptual visualization, Fig. 1a shows the experimental images obtained in the course of the present investigation for the suite of possible jet collision outcomes of *soft* merging (I), bouncing (II), and *hard* merging (III), with increasing impact inertia. Here, *soft* merging denotes merging attained at lower impact velocities, where impact inertia is weak to cause significant deformation of the circular jets, during the impact. *Hard* merging, on the other hand, is attained with high impact velocity or inertia, which causes significant deformation in the shape of the jet [17]. Further increase in impact inertia beyond III leads to instabilities that disintegrate the collided jet structure. Such instabilities and the ensuing atomization have been extensively studied in refs. [22, 23].

Recognizing the relevance of system pressure in automotive, airplane, and rocket engines, studies on droplet-droplet collision have also demonstrated that increasing pressure promotes bouncing because of the increased pressure- and hence density-dependent interfacial mass that needs to be displaced. Furthermore, because of the substantial differences in the physical properties between water and hydrocarbons, with water having a larger surface tension and stronger van der Waals force than alkanes, it was also shown that water droplets do not exhibit bouncing at atmospheric pressure, but they readily bounce at higher pressures. On the other hand, while hydrocarbon droplets bounce at atmospheric pressure, they merge at reduced pressures [9]. This property-dependent understanding is enlightening in that extensive investigations on hydrocarbon fuel spray processes for engine applications have inadvertently assumed droplet merging upon collision based on the results of water droplet collision at atmospheric pressure [24], and as such have led to biased spray statistics in analyzing engine combustion behavior.

In view of the above considerations, we have performed a systematic experimental investigation on obliquely oriented colliding jets under both elevated- and reduced-pressure environments. We shall show in due course that the resistance to bouncing for water jets differs from the hydrocarbon jets, as observed for the droplet collision [8, 9]. Furthermore, we have also identified a new phenomenon that, for a certain range of operations, merging instead of bouncing can be promoted at higher pressures, which is contrary to the results of droplet collision [9].

To achieve ambient pressure control of the jets, two identical nozzles, together with their relative position and orientation manipulation system, are placed in a sealed chamber with multiple observation windows in specific directions. A schematic of the experimental setup for the controlled-pressure jet collision experiments is shown in Fig. 1b.

* Email: asaha@eng.ucsd.edu

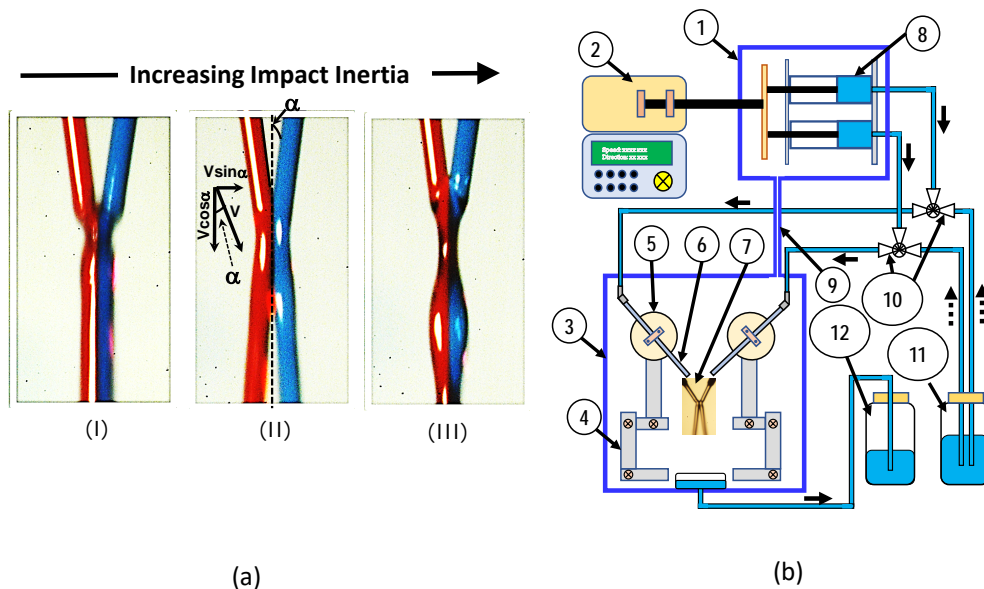


FIG. 1. (a) Images showing the suite of the collision response with increasing collision velocity (or impact inertia). (I): *soft* merging; (II): *bouncing*; (III): *hard* merging. Liquid: dyed n-tetradecane; pressure: 1 bar. (b) Schematic illustration of the experimental apparatus. 1. Syringe chamber; 2. Syringe pump controller; 3. Jet chamber; 4. XYZ-micro-position stage; 5. Micro-rotation stage; 6. Jet nozzle; 7. Quartz observation window; 8. Glass syringes; 9. Pressure balance connector; 10. Three-way valves; 11. Liquid reservoir; 12. Waste liquid reservoir.

A connected dual-chamber design keeps the pressure balance between the syringe chamber and the jet chamber so that the stability of the fluid flux generated from the pump can be guaranteed under different pressure conditions. With this setup, the test liquid is first drawn into the glass syringes from a liquid reservoir and then injected into the nozzles inside the jet chamber to form colliding jets after the chamber pressure is established. The flow rate of the system can be varied from 1.0 to 28.0 ml/min with an accuracy of $\pm 0.5\%$. Considering the extra pressure resistance from the pipes, adapters, and nozzles, the flux is calibrated under various pressure conditions, according to which the experimental results are further amended to keep the data accurate. Two identical nozzles with an inner diameter of 200 μm were designed by fixing the short thin-wall capillary tube inside a drilled copper column. Compared with the normally used glass capillary or needles, such nozzles yield sharper edges to avoid tip adhesive attraction of the liquid without increasing the pressure resistance and hence are able to generate fluid jets with a larger velocity range. The impact angle (α , shown in Fig. 1a) and position of the nozzles are precisely manipulated through micro-rotation and XYZ-micro-positioning, which can be conveniently controlled outside the chamber through soft driver connectors. Technical grade de-ionized water and n-tetradecane are used as the working fluids; their properties are listed in Table I.

TABLE I. Properties of the liquids used for the study

Liquid	density, ρ (kg/m^3)	dynamic viscosity, η ($10^{-3}\text{Pa}\cdot\text{s}$)	surface tension, σ ($10^{-3}\text{N}/\text{m}$)
Water (H_2O)	1000	1.01	72.90
n-Tetradecane (C14)	760	2.30	26.56

The bouncing behavior of n-tetradecane under the normal pressure (1 bar) condition is first investigated. By gradually varying the jet velocity and impact angle, we have mapped the regimes within which the collision yields (soft) merging, bouncing, and (hard) merging, with the bouncing outcome separating the soft and *hard* merging outcomes. Figure 2a maps the merging-vs-bouncing response of the colliding jets and shows the dependence of critical velocity delineating the transition with the collisional angle of the jets. The critical velocities generate two boundaries for *hard* and *soft* transitions, splitting the outcome into regimes I, II, and III. It is seen that the *soft* merging transition boundary is nearly insensitive to impact angle (α), having an almost constant critical velocity, while the *hard* merging transition boundary has a strong dependence on the impact angle, with a significant decrease in the critical velocity. These two transition boundaries merge at a certain angle (α_{cr}), 38° for n-tetradecane, beyond which bouncing is not observed. Similar transition boundaries are obtained for other alkanes, n-hexadecane, n-dodecane and n-decane,

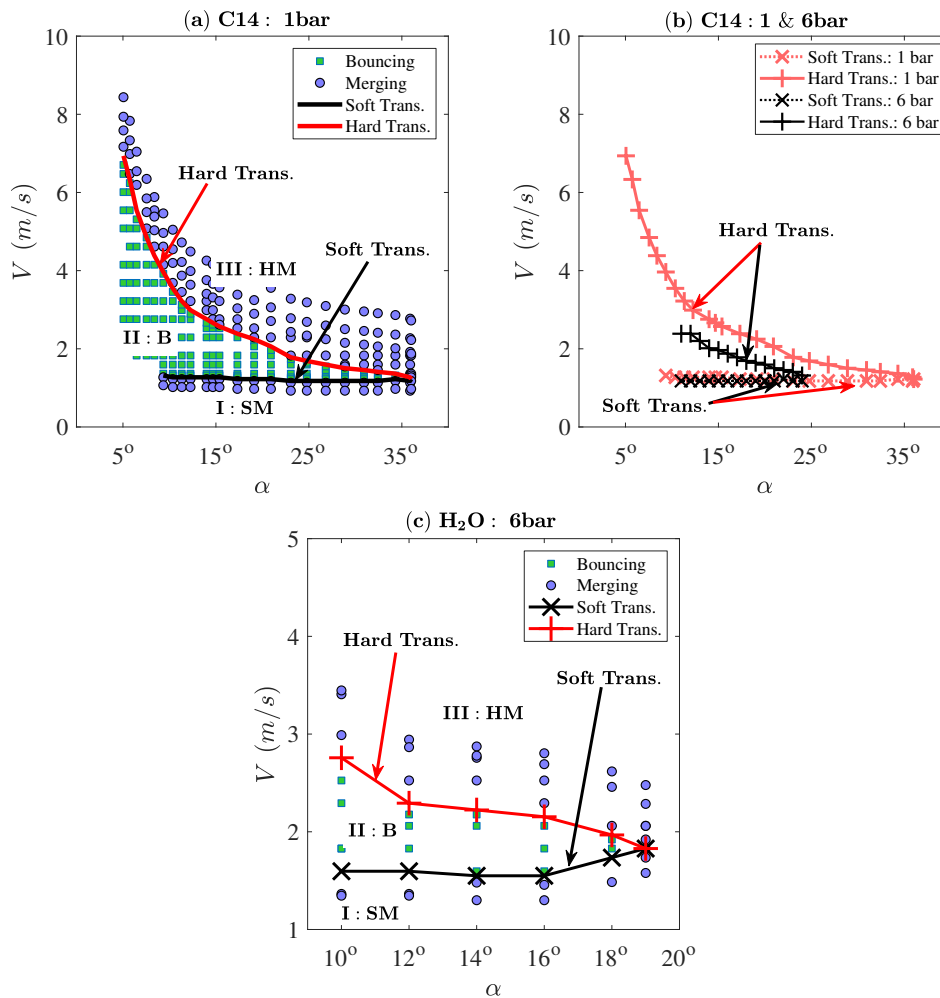


FIG. 2. (a) Regime map for n-tetradecane (C14) at 1 bar. (b) Comparison of regime boundaries for n-tetradecane (C14) at 1 bar and 6 bar. (c) Regime map for water (H₂O) at 6 bar. Various impact outcomes: bouncing, (*soft* and *hard*) merging and the (*soft* and *hard*) transition boundaries are shown. The data for n-tetradecane at 1 bar was presented in [17]. The uncertainty in V is about $\pm 5\%$. **SM**: soft merging; **B**: bouncing; **HM**: hard merging.

with α_{cr} being 44° , 28° and 19° respectively, as reported in our previous work [17]. In that work, we analyzed and showed that the *hard transition* boundary is dominated by the gas-layer thickness (H_d) evolution which scales as $H_d/R = A_I St^{-2/3}$, where $St = (\rho_l RU)/\eta_g$ is the Stokes number, A_I a prefactor, ρ_l the liquid density, R the jet radius, η_g the air viscosity and U the effective impact velocity which is $V \sin \alpha$ in the present case. The *soft transition* boundary is dominated by the Plateau-Rayleigh instability of the jet surface, leading to the velocity ratio, $\Gamma = V/V_c$, where $V_c = \sqrt{\sigma/(\rho_l R)}$ is the velocity of the capillary waves traveling along the jet and σ is surface tension.

Since the gas density can directly influence the inertia of the gas layer, it is straightforward to consider its effects by varying the gas pressure. First, to assess whether the pressure variation can affect the liquid side of the bouncing jet, we captured the jet shape and measured the characteristic geometry parameters, including the contact length, maximum deformation, and separation angle of the bouncing jets, respectively, under pressures from 1 to 6 bar. Results show that the shape evolution of the liquid jets has no visible dependence on the system pressure, which implies that, in this case, the ambient pressure variation has no effect on the liquid side during the jet bouncing process. This is to be expected because the viscosity and surface tension of the liquid barely change within this pressure range, and the density ratio between liquid and air, ρ_l/ρ_g , is over 500, which is much larger than the gas density variation. Consequently, the influence of pressure on the non-coalescence behavior of the jets could only play a role through the gas layer dynamics.

Subsequent extensive experimental investigations on jet collision in elevated and reduced pressure ambience were conducted, showing that, similar to droplet collision, no bouncing is observed for water jets under normal pressure (1 bar), and is exhibited at higher pressures, such as 6 bar as shown in Fig. 2c. For n-tetradecane jets, bouncing is

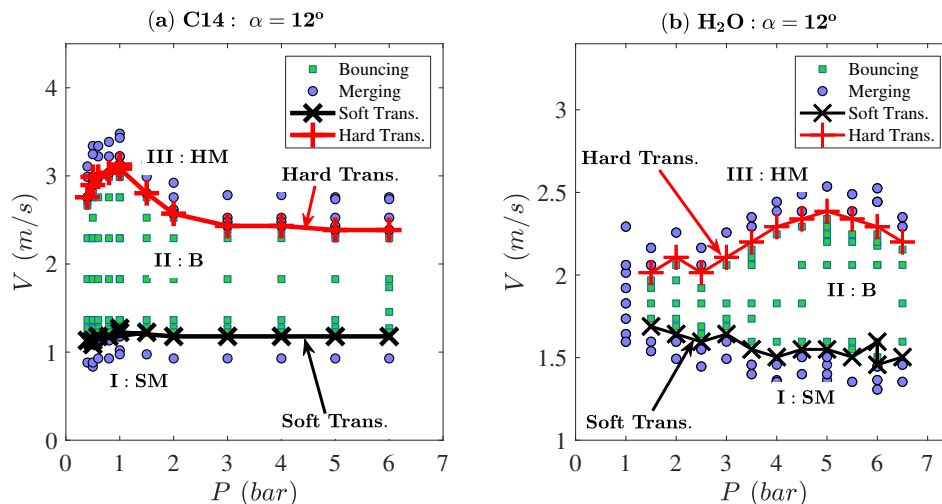


FIG. 3. Regime map as functions of the impact velocity and ambient pressure for (a) n-tetradecane (C14) and (b) Water (H_2O). Impact angle, $\alpha=12^\circ$. The uncertainty in V is about $\pm 5\%$. **SM**: soft merging; **B**: bouncing; **HM**: hard merging.

observed at normal pressure but is suppressed when the pressure is reduced to 0.2 bar. The investigation, however, identified an important qualitative difference between droplet and jet collisions at high pressures. With increasing impact inertia and within the range of higher pressures investigated, the *hard transition* boundary, from bouncing to *hard merging*, is reduced instead of expanded for n-tetradecane. As shown in Fig. 2b, the *hard transition* velocities at 6 bar are much smaller than those at 1 bar, leading to a narrower bouncing regime and rendering the critical collisional angle decreasing from 38° to 24° . To further explore and quantify this new phenomenon, additional experiments were conducted with water and n-tetradecane for various pressures while keeping the jet collision angle fixed at 12° . Figure 3 quantifies the non-monotonic behavior of the *hard transition* boundary with increasing pressure, first increasing and then decreasing, and hence promoting and inhibiting bouncing, respectively. For water jets, a small change in the *soft transition* boundary is also observed, in that it decreases slightly with increasing pressure (Fig. 3b). However, the non-monotonicity in *hard transition* boundary is more dramatic, and it controls the expansion/reduction in the bouncing regime. The transition state (from expansion to reduction in bouncing regime) occurs at a critical pressure P_{cr} of 0.9 bar for n-tetradecane (Fig. 3a) and 5 bar for water (Fig. 3b). Limited experiments with other impact angles at various pressures were also conducted. Although they were insufficient to draw complete regime maps at other impact angles, we observed similar behavior reported in Fig. 3.

In summary, we have identified the pressure effect on the jet-jet collision response. Unlike the widely investigated droplet-droplet collision case, pressurized ambient gas does not always promote bouncing in jet-jet collision. A unified non-monotonic trend of bouncing transition boundary is identified, leading to a critical pressure under which the collisional jets achieve maximum bouncing. The understanding gained, herein, yields a useful reference for practical applications, offering an additional consideration to the role of pressure on the bouncing versus coalescence of colliding jets. The experimental observations also serve as benchmark data for future theoretical and modeling expositions, which are required to provide additional details on the underlying interfacial dynamics.

-
- [1] W. Macklin and P. Hobbs, Subsurface phenomena and the splashing of drops on shallow liquids, *Science* **166**, 107 (1969).
 - [2] B. Ching, M. W. Golay, and T. J. Johnson, Droplet impacts upon liquid surfaces, *Science* **226**, 535 (1984).
 - [3] G. Falkovich, A. Fouxon, and M. Stepanov, Acceleration of rain initiation by cloud turbulence, *Nature* **419**, 151 (2002).
 - [4] I. V. Roisman and C. Tropea, Impact of a drop onto a wetted wall: description of crown formation and propagation, *J. Fluid Mech.* **472**, 373 (2002).
 - [5] W. Bouwhuis, R. C. van der Veen, T. Tran, D. L. Keij, K. G. Winkels, I. R. Peters, D. van der Meer, C. Sun, J. H. Snoeijer, and D. Lohse, Maximal air bubble entrainment at liquid-drop impact, *Phys. Rev. Lett.* **109**, 264501 (2012).
 - [6] T. Tran, H. de Maleprade, C. Sun, and D. Lohse, Air entrainment during impact of droplets on liquid surfaces, *J. Fluid Mech.* **726** (2013).
 - [7] A. Saha, Y. Wei, X. Tang, and C. K. Law, Kinematics of vortex ring generated by a drop upon impacting a liquid pool, *J. Fluid Mech.* **875**, 842 (2019).
 - [8] Y. Jiang, A. Umemura, and C. Law, An experimental investigation on the collision behaviour of hydrocarbon droplets, *J.*

- Fluid Mech. **234**, 171 (1992).
- [9] J. Qian and C. K. Law, Regimes of coalescence and separation in droplet collision, *J. Fluid Mech.* **331**, 59 (1997).
 - [10] P. Zhang and C. K. Law, An analysis of head-on droplet collision with large deformation in gaseous medium, *Phys. Fluids* **23**, 042102 (2011).
 - [11] C. Tang, J. Zhao, P. Zhang, C. K. Law, and Z. Huang, Dynamics of internal jets in the merging of two droplets of unequal sizes, *J. Fluid Mech.* **795**, 671 (2016).
 - [12] K. L. Pan and C. K. Law, Dynamics of droplet–film collision, *J. Fluid Mech.* **587**, 1–22 (2007).
 - [13] X. Tang, A. Saha, C. K. Law, and C. Sun, Nonmonotonic response of drop impacting on liquid film: mechanism and scaling, *Soft Matter* **12**, 4521 (2016).
 - [14] S. Shin, M. Li, X. Wu, A. Saha, and J. Bae, Role of soft-gel substrates on bouncing-merging transition in drop impact on liquid film, *Soft Matter* **17**, 571 (2021).
 - [15] X. Wu and A. Saha, Droplet impact on liquid films: bouncing-to-merging transitions for two-liquid systems, *Physics of Fluids* **34**, 103313 (2022).
 - [16] N. Wadhwa, P. Vlachos, and S. Jung, Noncoalescence in the oblique collision of fluid jets, *Phys. Rev. Lett.* **110**, 124502 (2013).
 - [17] M. Li, A. Saha, D. Zhu, C. Sun, and C. K. Law, Dynamics of bouncing-versus-merging response in jet collision, *Phys. Rev. E* **92**, 023024 (2015).
 - [18] G. P. Neitzel and P. Dell’Aversana, Noncoalescence and nonwetting behavior of liquids, *Ann. Rev. Fluid Mech.* **34**, 267 (2002).
 - [19] Y. Couder, E. Fort, C.-H. Gautier, and A. Boudaoud, From bouncing to floating: noncoalescence of drops on a fluid bath, *Phys. Rev. Lett.* **94**, 177801 (2005).
 - [20] S. T. Thoroddsen, M.-J. Thoraval, K. Takehara, and T. Etoh, Micro-bubble morphologies following drop impacts onto a pool surface, *J. Fluid Mech.* **708**, 469 (2012).
 - [21] X. Tang, A. Saha, C. K. Law, and C. Sun, Bouncing drop on liquid film: Dynamics of interfacial gas layer, *Phys. Fluids* **31**, 013304 (2019).
 - [22] J. W. Bush and A. E. Hasha, On the collision of laminar jets: fluid chains and fishbones, *J. Fluid Mech.* **511**, 285 (2004).
 - [23] N. Bremond and E. Villermaux, Atomization by jet impact, *J. Fluid Mech.* **549**, 273 (2006).
 - [24] P. O’Rourke and F. Bracco, Modeling of droplet interactions in thick sprays and a comparison with experiments: Startified Charge Auto. Eng. Conf., 101–115, *Inst. Mech. Eng. Pub. ISMB 0-85298-4693*.